

<i>Cryst. Res. Technol.</i>	35	2000	3	307–314
-----------------------------	----	------	---	---------

H. SAWADA

Department of Applied Chemistry, Kogakuin University, Tokyo, Japan

Estimation and Correction of Effects of Simultaneous Reflections on Intensity Data Collected with the Four-Circle Diffractometer

A procedure based on the kinematical theory has been developed to estimate and correct the effects of simultaneous reflections on intensity data collected with the four-circle single crystal X-ray diffractometer through minimizing the scatter of the corrected structure factor (intensity) values of equivalent reflections.

Keywords: simultaneous reflection, multiple reflection, multiple diffraction, Renninger effect, four-circle diffractometer, X-ray diffraction

(Received June 22, 1999; Accepted January 10, 2000)

Introduction

Simultaneous reflection, also termed multiple reflection or multiple diffraction, is virtually inherent in X-ray diffraction experiments, which can be expected to occur without exception when one or more lattice planes other than that being oriented for intensity measurements also satisfy the diffraction condition. This situation is equivalent to additional reciprocal points being situated simultaneously on the Ewald sphere at the instant the reciprocal point under consideration is being measured.

If the Miller indices of the reflection currently under measurement, and those of the second reflection on the Ewald sphere are represented as \mathbf{h}_1 and \mathbf{h}_2 , respectively, the condition for simultaneous reflection becomes $\mathbf{h}_1 = \mathbf{h}_2 + \mathbf{h}_3$, where the third set of indices represents an additional reflection mediating the interactions between \mathbf{h}_1 and \mathbf{h}_2 with either once-reflected beam acting as the incident beam.

The treatment of simultaneous reflection in the present report is based on kinematical interactions between these three reflected beams; for any case of a multiple-beam interaction, it will be treated as a sum of three-beam interactions. Interference between beams will not be considered. Phase relations cannot be ignored when near-to-perfect crystals are used and the incident beam has small divergence, as does sufficiently monochromatized and collimated synchrotron radiation. However, provided that the X-ray apparatus used is a conventional one, the kinematical treatment is believed to be valid. The kinematical approach has been both treated theoretically and applied to experiment in [MOON *et al.*]. The three-beam scheme has been found to be effective in simulating ψ -scan profiles of simultaneous reflections [SOEJIMA *et al.*].

It has been reported [TANAKA *et al.*] that for carefully measured intensities for equivalent reflections, the chief cause of their differences in intensity is the effect of simultaneous reflection. This will, in turn, be taken as an advantage in the present study, in evaluating the magnitude of the effect.

Most, if not all previous works employ the ψ -scan technique in demonstrating the detection of simultaneous reflections. The focus of the present procedure is on estimation and correction of affected intensity data routinely collected by a four-circle diffractometer through the ω -moving kind of scan, without any kind of additional checks to be made by ψ -scanning.

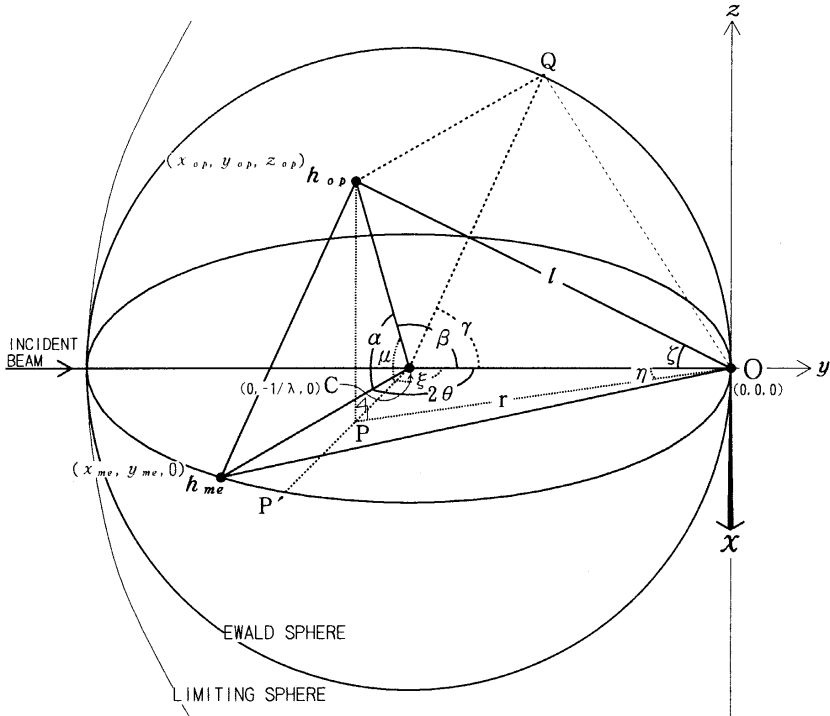


Fig. 1: The geometry of the experimental setup and the three-beam scheme

Calculation Procedures

When the matrix transforming a point with indices h on a reciprocal lattice to a set of Cartesian coordinates fixed on the reciprocal lattice is B , and the relation of Bh with the laboratory coordinates is given by U , the laboratory coordinates of a reciprocal lattice point becomes $(x_l, y_l, z_l) = UBh$. In the present experimental setup, the direction of the incident X-rays corresponds to y , the direction perpendicular to y and in the plane of observation: x , and the direction perpendicular to the xy -plane: z (Fig.1). Rotation of this reciprocal lattice point around the machine axes according to the orientation of another lattice point presently being measured is considered, and the resulting position of h is checked whether it is on the Ewald sphere. Let Φ , X , and Ω represent the rotations around the ϕ , χ , and ω axes, respectively. Then, the coordinates for the rotated lattice point becomes:

$$(x, y, z)_{rotated} = \Omega X \Phi U B h . \tag{1}$$

Since the origin of the limiting sphere of observation O (which is also the origin of the reciprocal crystal lattice) is the farther intersecting point of the incident X-ray and the Ewald sphere, the coordinates of the center of the Ewald sphere C where the crystal is set is

(0, $-1/\lambda$, 0). The coordinates of the reciprocal lattice point corresponding to the reflection currently being measured \mathbf{h}_{me} is $(x_{me}, y_{me}, 0)$; that of the second lattice point on the Ewald sphere: (labeled as in [SOEJIMA *et al.*],) the *operative point* \mathbf{h}_{op} , is at (x_{op}, y_{op}, z_{op}) , and the projection of \mathbf{h}_{op} onto the xy plane \mathbf{P} is $(x_{op}, y_{op}, 0)$, its distance from \mathbf{O} : $r = (x_{op}^2 + y_{op}^2)^{1/2}$. Point \mathbf{Q} $(x_{op} - x_{me}, y_{op} - y_{me}, z_{op})$ is used to derive the angle between the incident beam and the lattice point of the third reflection connecting the first two, the *cooperative point*; \mathbf{h}_{co} : corresponding to a vector connecting \mathbf{h}_{op} to \mathbf{h}_{me} . The angles used for the subsequent calculations are the following: $\alpha = \angle \mathbf{h}_{me} \mathbf{C} \mathbf{h}_{op}$, $\beta = \angle \mathbf{O} \mathbf{C} \mathbf{h}_{op}$, $\gamma = \angle \mathbf{O} \mathbf{C} \mathbf{Q}$, $\zeta = \angle \mathbf{C} \mathbf{O} \mathbf{h}_{op}$, $\eta = \angle \mathbf{C} \mathbf{O} \mathbf{P}$, $\mu = \angle \mathbf{P} \mathbf{C} \mathbf{h}_{op}$, $\xi = \angle \mathbf{O} \mathbf{C} \mathbf{P}$ (Fig.1).

Reciprocal points situated within a certain distance from the Ewald sphere surface are taken into account, and included in the subsequent calculations. A shell of finite thickness is considered, bounded by spheres slightly smaller and larger than the Ewald sphere. Accordingly, the effective Lorentz factor L can be calculated from the time it requires to pass through this shell. The present procedure defines an inner bordering sphere with radius $1/\lambda(1+\Delta)$, and an outer bordering sphere with radius $1/\lambda(1-\Delta)$. The centers of these spheres are at $y = -\delta - [1/\lambda(1+\Delta)]$ and $y = \delta - [1/\lambda(1-\Delta)]$, respectively, with $x=0$, $z=0$. When $\delta=0$, the surfaces of the two spheres touch each other at \mathbf{O} , while the shell thickness becomes constant for all directions for the concentric case when $\delta = \Delta/\lambda(1-\Delta^2)$. The shell thickness can be regarded as indicating the effective profile width showing effects of divergence and wavelength dispersion of the X-rays. The Δ value should not be taken too wide such as to put the entire diffraction profile within the shell thickness, since effects other than the aforementioned also contribute to the widening of the profile. The value: $\Delta=0.001$ was chosen in the present study, which corresponds roughly to the half widths of the profiles. An appropriate δ value may be derived from the diffraction profile widths of reflections at various diffraction angles. If it is chosen *not* to assume the concentric case, it may be necessary for the Lorentz factor, used to reduce the measured intensities to the observed structure factor values, to be recalculated (depending on the degree of consistency required between the Lorentz schemes for the measured observations and the corrections). For this study, recalculation was not considered, since the preponderance of the intensifying effect on the diffraction intensity due to diffraction profile broadening, against the diminution caused by reduction of the profile height, could not be evaluated with the present procedures.

The velocity of the reciprocal point is proportional to its distance from the z axis which is the axis of revolution for the ω -moving type scanning mode: $v=2\sin\theta$ for \mathbf{h}_{me} , $v=r\lambda$ for \mathbf{h}_{op} . The correction considering the difference between the direction of the passage and the radial direction of the Ewald sphere is given by $\cos\theta$ for \mathbf{h}_{me} , $\sin(\eta+\xi)\cos\mu$ for \mathbf{h}_{op} taking into consideration the general case where \mathbf{h}_{op} is vertically offset from the xy plane.

The shell thickness (\AA^{-1}) at the measured and operative point positions become:

$$\vartheta_{me} \cong [2\Delta / \lambda(1-\Delta^2)] [2(1-d)\sin^2\theta + d] \quad (2)$$

$$\vartheta_{op} \cong [2\Delta / \lambda(1-\Delta^2)] [2(1-d)\cos^2\zeta + d] \quad (3)$$

where $d = [\lambda(1-\Delta^2)/\Delta]\delta$, thus $0 \leq d (\leq 2; d=0.55$ for the example shown later). From analogy to its definition in the conventional case, we can proceed to derive the Lorentz factors:

$$L_{me} \cong [2(1-d)\sin^2\theta + d] / \sin 2\theta \quad (4)$$

$$L_{op} \cong [2(1-d)\cos^2\zeta + d] / r\lambda\sin(\eta+\xi)\cos\mu \quad (5)$$

In the grazing-entry case, \mathbf{h}_{op} follows a path that barely skims the outer sphere without passing inside the inner sphere, satisfying either of the following relations:

$$1 - \sin\mu \leq \Delta / (1 - \Delta^2), \quad (6a)$$

$$r \geq | - \{ 1 / \lambda^2 (1 + \Delta)^2 \} - z_{op}^2 \}^{1/2} - [1 / \lambda (1 + \Delta)] - \delta |, \quad (6b)$$

$$r \leq | \{ 1 / \lambda^2 (1 + \Delta)^2 \} - z_{op}^2 \}^{1/2} - [1 / \lambda (1 + \Delta)] - \delta |. \quad (6c)$$

The path length of the reciprocal point is derived from the intersects of the outer sphere and the circle $x_{op}^2 + y_{op}^2 = r^2$ on plane z_{op} :

$$y_{op} = [\lambda(\Delta - 1)(r^2 + z_{op}^2 - \delta^2) + 2\delta][1 + \delta\lambda(\Delta - 1)] / 2 \quad (7a)$$

$$x_{op} = \pm (r^2 - y_{op}^2)^{1/2}. \quad (7b)$$

The path length becomes $\vartheta_{op}' (\text{\AA}^{-1}) \cong 2r \tan |x_{op} / y_{op}|$. Since the expression for the velocity of this point is the same as the normal case: $v = r\lambda$, the Lorentz factor becomes:

$$L_{op} = [\lambda(1 - \Delta^2) / 2\Delta] \vartheta_{op}' / v \cong [(1 - \Delta^2) / \Delta] \tan |x_{op} / y_{op}|. \quad (8)$$

The path length derived above becomes approximately twice that of the normal case near the grazing entry limit, since it extends to the opposite side of the outer sphere. An additional function needs to be attached in order to give a gradual change from the grazing incident limit to the most extreme case in which the reciprocal point touches the remotest part of the Ewald sphere and the path length derived above becomes fully valid.

Furthermore, since operative points lying within a certain range of distance from the surface of the ideal Ewald sphere are included in the calculations, the degree of contribution from each operative point must be evaluated. Some cases may be seen as a span of time between the occurrences of the two reflections, while in others, the operative point simply may not touch the ideal Ewald sphere at all. Moreover, the scan position and width for the actually measured reflection is set to accommodate the profile of h_{me} ; therefore, the *effective* profile of h_{op} in terms of synchronicity with the measured profile of h_{me} must be procured. The expressions for L_{op} derived above cannot be used straightforwardly in adjusting the intensity of h_{op} .

In the present procedure, the reflected fraction of the incident beam intensity is derived for each scan position of h_{me} divided into small intervals along with those at the corresponding positions of h_{op} . The ratio between the distance of a reciprocal point from the Ewald sphere surface against the shell thickness at that position (indicating the effective size of the diffraction spot (\equiv reciprocal point with finite size)) is used as a measure to its contribution to the reflection. Assuming a Gaussian intensity distribution for the diffraction spot, this method also accounts for the deviation of the scanned profile from a Gaussian form due to the general asymmetry seen in its path with respect to the Ewald sphere surface.

The displacement σ of h_{me} or h_{op} from the surface of the Ewald sphere is determined from its coordinates at each interval:

$$\sigma_{(u)} = | [x_{(u)}^2 + (y_{(u)} + 1/\lambda)^2 + z_{(u)}^2]^{1/2} - 1/\lambda | \quad (9)$$

$$(x_{(u)}, y_{(u)}, z_{(u)}) = \Omega_{(u)} X \Phi U B h. \quad (1')$$

The rotation $\Omega_{(u)}$ gives the ω position at an instant in the scanning of h_{me} or the corresponding position of h_{op} :

$$\omega_{(u)} = \omega + [(u+1)/2 - offs](a + b \tan\theta), \quad (10)$$

The range of u is taken to be $-1 \leq u \leq +1$. The parameters a and b give the scan width, *offs* (usually ≈ 0.5) the scan offset in the measurement. As mentioned before, these scan

parameters are normally chosen so that the entire measured profile is brought into the scanning range, thus are generally taken to be considerably wider than the effective profile width. For the characteristic MoK radiation used in the example, for instance, the α_1 and α_2 peaks are inseparable at low angles, so contributions from both are included in the integrated intensity. (Tacit antecedents when using a characteristic X-ray source become evident; that there are no crossover interactions between coexisting radiations even at high angles where they become distinguishable, and their degrees of contribution to the integrated intensity are constant throughout the measured data.)

The expression for the cooperative point is also derived. Either the \mathbf{h}_{me} or \mathbf{h}_{op} beam acting as the incident for the diffraction towards the direction of the other beam results in the \mathbf{h}_{co^*} or \mathbf{h}_{co} beam. Thus, the product of the contributions from \mathbf{h}_{me} and \mathbf{h}_{op} for the corresponding interval becomes the fraction of incident radiation reflected as the cooperative beam.

The fractions of the incoming uniform incident intensity reflected per unit reflectivity at each interval are represented by:

$$E_{me} = \exp[-m(2\sigma_{(u)me} / \vartheta_{me})^2], \quad (11)$$

$$E_{op} = \exp[-m(2\sigma_{(u)op} / \vartheta_{op})^2]. \quad (12)$$

The overall fractions are given by the following:

$$s_{me} = \int E_{me} du / \int du, \quad (13)$$

$$s_{op} = \int E_{op} du / \int du, \quad (14)$$

$$s_{co} = s_{co^*} = \int E_{me} E_{op} du / \int du. \quad (15)$$

In the actual calculations for the present work, the integrals were replaced by summation for 201 intervals, while the "sharpness" m of the Gaussian function taken to be ≈ 2 brought satisfactory results for $\Delta=0.001$ within minimum extent of the shell thickness.

The s values already incorporate the speed-and-direction-of-passage effect (the Lorentz factor) ratios with respect to L_{me} , since each corresponding degree of contribution is accounted for the same number of intervals each.

The polarization factor has been dealt with in several previous studies [AZAROFF; MOON *et al.*; ZACHARIASEN; SOEJIMA *et al.*]. Assuming an unpolarized incident beam and defining an auxiliary angle as in [AZAROFF] with the present angles:

$$\rho = \cos^{-1}[(\cos\gamma - \cos 2\theta \cos\alpha) / \sin 2\theta \sin\alpha], \quad (16)$$

the polarizing factor for \mathbf{h}_{co} is:

$$p_{co} = [(\cos^2\beta \cos^2\rho + \sin^2\rho) \cos^2\alpha + \cos^2\beta \sin^2\rho + \cos^2\rho] / (1 + \cos^2\beta); \quad (17)$$

that for \mathbf{h}_{co^*} which corresponds to the same beam propagating to the opposite direction becomes:

$$p_{co^*} = [(\cos^2 2\theta \cos^2\rho + \sin^2\rho) \cos^2\alpha + \cos^2 2\theta \sin^2\rho + \cos^2\rho] / (1 + \cos^2 2\theta). \quad (18)$$

Obviously,

$$p_{me} = (1 + \cos^2 2\theta) / 2, \quad (19)$$

and as can be seen from the geometrical correspondence of \mathbf{h}_{op} with \mathbf{h}_{me} (Fig.1),

$$p_{op} = (1 + \cos^2\beta) / 2. \quad (20)$$

The incident intensity which is reflected as \mathbf{h}_{me} is diminished to a certain extent; as the incident beam, encountering *two* different lattice planes simultaneously satisfying the

diffraction condition, gives away fractions of intensity to *both* \mathbf{h}_{me} and \mathbf{h}_{op} ; fractions which are related to their total reflecting powers. The beam \mathbf{h}_{me} itself is also subjected to further intensity reduction due to a secondary reflection occurring after it is once reflected: \mathbf{h}_{co^*} , which shaves off some extra intensity before it arrives at observation. These diminishing effects on the observed intensity are termed *Aufhellung*. On the other hand, intensity also flows *into* \mathbf{h}_{me} out of \mathbf{h}_{op} via \mathbf{h}_{co} ; resulting in a brightening effect, *Umweganregung* on \mathbf{h}_{me} . The intensities \mathbf{G} 's that determine the magnitudes of interactions between these three beams (moving toward four directions) are related to their structure factors \mathbf{F} 's:

$$\mathbf{G}_{me} = |\mathbf{F}_{me}|^2 \mathbf{L}_{me} \mathbf{p}_{me}, \quad (21a)$$

$$\mathbf{G}_{op} = |\mathbf{F}_{op}|^2 \mathbf{L}_{op} \mathbf{p}_{op}, \quad (21b)$$

$$\mathbf{G}_{co} = |\mathbf{F}_{co}|^2 \mathbf{L}_{co} \mathbf{p}_{co}, \quad (21c)$$

$$\mathbf{G}_{co^*} = |\mathbf{F}_{co^*}|^2 \mathbf{L}_{co^*} \mathbf{p}_{co^*}. \quad (21d)$$

Assuming that such effects as absorption and secondary extinction already have been corrected, the relation between the measured and calculated intensities when there are no considered effects of simultaneous reflection is represented by:

$$I_C = k \mathbf{G}_C = k |\mathbf{F}_C|^2 \mathbf{L}_{me} \mathbf{p}_{me} \quad (22)$$

where $k = I_{me} s_{me} \mathbf{R}$; \mathbf{R} : the reflectivity. Intensity values calculated from the tentatively refined parameters are used (with subscript c) for the primary reflection instead of the observed values. The calculated structure factors: \mathbf{F}_C 's used in these calculations are generated for reflections within the entire range of the limiting sphere of observation.

The intensity of a reflection affected by multiple-occurring simultaneous reflections, treated as the sum of three-beam interactions becomes:

$$I'_C = I_{me} \mathbf{R} [\mathbf{G}_C (s_{me} - \mathbf{R} \sum s_{op(i)} \mathbf{G}'_{op(i)}) - s_{me} \mathbf{R} \mathbf{G}_C \sum s_{co(i)} \mathbf{G}'_{co^*(i)} + \mathbf{R} \sum s_{op(i)} s_{co(i)} \mathbf{G}'_{op(i)} \mathbf{G}'_{co(i)}]. \quad (23)$$

The s values for the operative and cooperative reflections indicate the synchronicity relative to s_{me} , so the Lorentz factors for \mathbf{h}_{op} , \mathbf{h}_{co} and \mathbf{h}_{co^*} are all reset equal to \mathbf{L}_{me} , their intensities indicated by \mathbf{G}' . Without the synchronicity relations, this equation is identical to that given in [SOEJIMA *et al.*], extended to a multiply occurring 3-beam case.

The structure factor with the combined effects of all considered contributions from simultaneous reflections included takes the form:

$$|\mathbf{F}_{C(comb)}|^2 = I'_C / k \mathbf{L}_{me} \mathbf{p}_{me}, \quad (24)$$

and the correction becomes:

$$\mathbf{F}_{me(corr)} = \mathbf{F}_{me} |\mathbf{F}_C| / |\mathbf{F}_{C(comb)}|. \quad (25)$$

The reflectivity value giving the correction with the least scatter among the $\mathbf{F}_{me(corr)}$ values is adopted as the reflectivity for that set of equivalents. High-symmetry structures enable comparison of observed structure factor values of equivalent reflections, which should essentially be close to equal if unaffected by simultaneous reflections. On the other hand, structures with low symmetry offer only limited numbers of equivalent reflections, and the chance for corrections being made mistakenly becomes high. However, the reflectivity values were seen to show a distribution maximum centered at a likely value, along with those at large and small values, the former indicating for the most part coincidental or ill-conditioned corrections, while the latter implies estimates giving insignificantly small corrections. Calculations using a single, most probable reflectivity value derived from the entire data, or, setting this value as the maximum permitted reflectivity, would be possible steps that can be taken in these cases. Furthermore, appropriate geometric considerations

coupled with a reliable reflectivity value would enable estimation of the effects of simultaneous reflection on data acquired with other techniques, such as the powder method.

Example of Application

An example of this procedure applied to structure factor data of a garnet-structured compound ($\text{Pr}_3\text{Ga}_5\text{O}_{12}$) collected with a four-circle single-crystal diffractometer (RIGAKU AFC6S) is presented. Full description of the structure is to be given elsewhere.

Data for up to 8 equivalents were collected. The structure was refined up to the anisotropic temperature factors. For each observed reflection, those fulfilling the general rules of systematic extinction for the space group: [$Ia\bar{3}d$, $a=12.544(1)\text{\AA}$, $h+k+l=2n$, $\text{MoK}\alpha$ radiation ($\lambda=0.71069\text{\AA}$, 84448 reflections)], including zero- F_c reflections; were checked as to whether they come close enough to the Ewald sphere and contribute to simultaneous reflections. There were only five sets of equivalents showing significantly large scatter of the structure factor values, which were all attributable, by use of this procedure, to prominent *Umweganregung* effects. Some strong reflections showed *Aufhellung*, though insignificant compared to standard deviations from counting statistics or averaging of the equivalents. Most of the reliable reflectivity values in garnet are distributed at around $R=10^{-9}$. The use of a single overall reflectivity seemed to be adequate; it could not be determined whether there are any secondary systematic trends in the refined reflectivity values with respect to scattering angle, intensity, etc. Values for $d=0.5\sim 0.6$ ($d=0.55$ used in the results shown) gave the best results for these selected sets of equivalents, in terms of scatter of the structure factor values. Selected results of the correction are shown in Tables 1-2.

It has been shown that the present procedure efficiently estimates simultaneous reflection effects. Trials on a spinel-structured compound and diamond exhibited similarly satisfactory results. Future structural studies employing this method are expected to help verify further the validity of this method.

n	h_{mc}	k_{mc}	l_{mc}	$F_{m(corr)}$	F_{mc}	F_c	dif.	R
62	8	2	0	11.35	12.77	70.34	-0.0590	0.42E-09
57	8	0	2	13.87	35.08	70.34	-0.4334	0.42E-09
75	0	-8	-2	13.29	13.37	70.34	-0.0029	0.42E-09
75	0	8	2	14.35	14.45	70.34	-0.0029	0.42E-09
57	-8	0	-2	13.78	34.86	70.34	-0.4334	0.42E-09
64	-8	2	0	15.53	15.64	70.34	-0.0036	0.42E-09
64	8	-2	0	14.21	14.31	70.34	-0.0036	0.42E-09
62	-8	-2	0	12.09	13.60	70.34	-0.0590	0.42E-09
59	-8	-6	-6	26.45	26.64	149.40	-0.0036	0.67E-09
62	-6	-8	-6	25.34	26.71	149.40	-0.0263	0.67E-09
62	8	-6	-6	28.04	35.63	149.40	-0.1193	0.67E-09
64	-6	8	6	25.91	25.86	149.40	+0.0009	0.67E-09
59	8	6	6	28.82	29.03	149.40	-0.0036	0.67E-09
64	6	-8	-6	23.89	23.85	149.40	+0.0009	0.67E-09
62	6	8	6	25.59	26.97	149.40	-0.0263	0.67E-09
62	-8	6	6	24.06	30.57	149.40	-0.1193	0.67E-09
63	10	-6	-2	6.53	12.78	47.19	-0.3236	0.92E-09
58	-10	-6	-2	9.06	27.60	47.19	-0.5060	0.92E-09
73	2	10	6	10.83	11.08	47.19	-0.0111	0.92E-09
58	10	6	2	9.32	28.40	47.19	-0.5060	0.92E-09

63	-10	6	2	6.73	13.18	47.19	-0.3236	0.92E-09
73	-2	-10	-6	6.31	6.45	47.19	-0.0111	0.92E-09
71	-10	-8	-2	18.88	21.68	111.73	-0.0691	0.83E-09
65	2	10	8	19.60	19.73	111.73	-0.0034	0.83E-09
71	-10	8	2	19.09	19.11	111.73	-0.0005	0.83E-09
71	10	8	2	19.30	22.16	111.73	-0.0691	0.83E-09
71	10	-8	-2	20.01	20.03	111.73	-0.0005	0.83E-09
59	10	2	8	18.15	18.16	111.73	-0.0003	0.83E-09
59	-10	-2	-8	18.35	18.36	111.73	-0.0003	0.83E-09
65	-2	-10	-8	19.36	19.49	111.73	-0.0034	0.83E-09
53	0	-20	-4	12.87	22.58	67.60	-0.2740	0.21E-08
66	-20	4	0	12.35	12.77	67.60	-0.0169	0.21E-08
66	20	-4	0	11.99	12.40	67.60	-0.0169	0.21E-08
53	0	20	4	11.79	20.69	67.60	-0.2740	0.21E-08
55	20	0	4	12.04	13.42	67.60	-0.0543	0.21E-08
43	-20	-4	0	12.20	12.57	67.60	-0.0148	0.21E-08
43	20	4	0	12.32	12.69	67.60	-0.0148	0.21E-08
55	-20	0	-4	12.80	14.27	67.60	-0.0543	0.21E-08

Table 1: List of selected equivalent reflections showing strong effects of simultaneous reflections. "n" is the number of three beam interactions, "dif.": the amount $(F_{me(corr)} - F_{me}) / (F_{me(corr)} + F_{me})$.

h_{op}	k_{op}	l_{op}	F_{op}	h_{co}	k_{co}	l_{co}	F_{co}	$\sigma(\text{\AA}^{-1})$	dif.	$F_{me(corr)}$
4	-30	2	165.50	4	30	0	232.63	+0.00003	-0.0010	35.01
4	-24	8	251.42	4	24	-6	307.39	-0.00081	-0.0070	34.59
4	-6	8	764.06	4	6	-6	729.92	-0.00082	-0.1318	26.91
4	0	2	1150.16	4	0	0	1056.91	+0.00002	-0.3688	16.18
12	-30	0	176.64	-4	30	2	165.50	+0.00090	-0.0002	35.07
12	-22	8	279.60	-4	22	-6	266.39	-0.00022	-0.0032	34.86
12	-8	8	435.63	-4	8	-6	764.06	-0.00023	-0.0684	30.59
12	0	0	507.49	-4	0	2	1150.16	+0.00088	-0.1225	27.42

Table 2: Selected individual 3-beam contributions significantly affecting the structure factor value of the 8 0 2 reflection in Table 1. The displacement of h_{op} from the Ewald sphere surface: $\sigma = [x_{oo}^2 + (y_{oo} + 1/\lambda)^2 + z_{oo}^2]^{1/2} - 1/\lambda$; $F_{me(corr)}$ values for each of the 3-beam interactions are shown.

References

- AZAROFF, L.V.: Acta Crystallogr. **8** (1955) 701
 MOON, R.M., SHULL, C.G.: Acta Crystallogr. **17** (1964) 805
 SOEJIMA, Y., OKAZAKI, A., MATSUMOTO, T.: Acta Crystallogr. **A41** (1985) 128
 TANAKA, K., SAITO, Y.: Acta Crystallogr. **A31** (1975) 841
 ZACHARIASEN, W.H.: Acta Crystallogr. **18** (1965) 705

Contact information:

Haruo SAWADA
 Department of Applied Chemistry, Kogakuin University
 2665-1 Nakano-machi, Hachioji, Tokyo 192-0015
 Japan

e-mail: sawada@cc.kogakuin.ac.jp